NASA TECHNICAL MEMORANDUM

NASA TM X-72663

NASA TM X-72663

WIND TUNNEL INVESTIGATION OF A 14' VERTICAL AXIS WINDMILL

by R. J. Muraca and R. J. Guillotte

This informal documentation medium is used to provide accelerated or special release of technical information to selected users. The contents may not meet NASA formal editing and publication standards, may be revised, or may be incorporated in another publication.

NATIONAL AERONAUTICS AND SPACE ADMINISTRATION

LANGLEY RESEARCH CENTER, HAMPTON, VIRGINIA 23665

1. Report No.	2. Government Accession No.	3. Recipient's Catalog No.
NASA TM X-72663		

4. Title and Subtitle	5. Report Date
Wind Tunnel Investigation of a 14' Vertical Axis Windmill	March 1976
	6. Performing Organization Code

7. Author(s)	8. Performing Organization Report No.
Ralph J. Muraca Robert J. Guillotte	
9. Performing Organization Name and Address	10. Work Unit No.
NASA Langley Research Center Hampton, VA 23665	11. Contract or Grant No.
12. Sponsoring Agency Name and Address	13. Type of Report and Period Covered
National Aeronautics & Space Administration Washington, DC 20546	Technical Memorandum
	14. Sponsoring Agency Code

15. Supplementary Notes

16. Abstract

An exploratory investigation was made in the Langley Research Center Full Scale Wind Tunnel to determine the performance characteristics of a 14' diameter vertical axis windmill. The parameters measured were wind velocity, shaft torque, shaft rotation rate, along with the drag and yawing moment. A velocity survey of the flow field downstream of the windmill was also made. The results of these tests along with some analytically predicted data are presented in the form of generalized data as a function of tip speed ratio.

17. Key Words (Suggested by Author(s))	18. Distribution Statement
Windmill, Vertical Axis Windmill, Energy	Unclassified - Unlimited

19. Security Classif. (of this report)	20. Security Classif. (of this page)	21. No. of Pages	22. Price*
Unclassified	Unclassified	31	$3.75

*For sale by the National Technical Information Service, Springfield, Virginia 22161

WIND TUNNEL INVESTIGATION OF A 14' VERTICAL AXIS WINDMILL

SUMMARY

An exploratory investigation has been made in the Langley Research Center Full Scale Wind Tunnel to determine the performance characteristics of a 14 Foot (4.267 m) diameter Vertical Axis Windmill. Tests were made over two ranges of free stream wind velocity. The parameters measured were wind velocity, shaft torque, shaft rotation rate, along with the drag and yawing moment of the windmill plus supporting structure. A velocity survey of the flow field downstream of the windmill was also made at one operating condition.

The results of these tests along with some analytically predicted data are presented in this report in the form of generalized data as a function of tip speed ratio. Good agreement was obtained between the experimental and analytical results.

INTRODUCTION

One of the areas of current interest in seeking alternate energy sources involves the use of windmills to convert wind energy to some useful form. The most familiar configuration is the horizontal axis type having sails or propellor type blades as the driven members, and an orientation device to align the axis parallel to the free stream.

Another type or windmill not quite as familiar is the vertical axis type. Unlike a conventional windmill, the axis of revolution is perpendicular to the mean wind velocity vector. This principle was patented by G.J.M. Darrieus, ref. 1.

The vertical axis windmill represents a potentially simple and low cost wind energy conversion device. The potential for cost saving derives from several aspects of the basic design. First, the axis of the windmill is vertical thus allowing direct shafting to generating equipment which may be located on the ground. This allows a lighter weight support structure. Secondly, although an airfoil shape is required for the blades to obtain good performance, the blades do not require twisting and mass production of the blades appears to be economically feasible. Third, the windmill is omni-directional with respect to wind direction thus it does not require a mechanism to maintain any particular orientation with respect to the wind direction. Fourth, the major blade loads are caused by centrifugal forces which are essentially steady in nature thus material fatigue should not be as severe a problem. The classical vertical axis concept does have one major disadvantage in that it is not self-starting and requires some device to restart it when prevailing winds drop below the threshold level.

The purpose of this report is to present the operating characteristics of one vertical axis windmill design. This configuration was chosen since some data had been obtained by South and Rangi, references 2 and 3, thereby allowing correlations to be made.

The variables measured were shaft torque, rotation rate, wind velocity, total drag, total torque, and velocity distributions in the wake of the windmill. These data have been reduced and presented in the form of power coefficient, drag coefficient and torque coefficient. Also included are typical results from reference 3 and some analytical results from ref. 4.

SYMBOLS

A	Windmill Swept Area, ft.^{2} (m^2)
C_p	Power Coefficient (see eq. (1)), Unitless
C_T	Torque Coefficient (see eq. (3)), Unitless
N	Windmill Rotation Rate, RPM
q_∞	Free-Stream Dynamic Pressure lb/ft.^{2} (n/m^2)
R	Windmill Tip Speed/Free-Stream Velocity (see eq. (2)), Unitless
r_{max}	Windmill Radius, Maximum, ft. (m)
T	Torque, in-lb (n-m)
V_∞	Free-Stream Wind Velocity, ft./sec (m/sec)
ρ	Mass Density, lb-sec^2/in^4 (K - sec^2/m^4)
ω	Angular Velocity, Windmill Rad/sec

APPARATUS & METHODS

TUNNEL

The tests were conducted in the Langley Research Center Full Scale Wind Tunnel. Physical and operating characteristics of this facility are given in reference 5.

MODEL

The test model was a two bladed Vertical Axis Windmill using the NACA 0012 airfoil and having a maximum diameter of 14 feet (4.267 m). Physical dimensions are shown in figure 1. The blade shape dimensions are shown on figure 2, and the ordinates of the NACA 0012 airfoil are shown on figure 3. A comnlete description of the test model including structural analysis is given in reference 6.

The blades used on the test configuration varied somewhat from a true NACA 0012 airfoil shape. This variation is due to the blade being originally constructed as a check on high strength-to-weight fabrication techniques, thus, it was not built to close tolerances. The average blade chord was 5.58 (0.0142 m) inches rather than 6 inches (0.0152 m) and the average thickness was 15% as opposed to 12%. In addition one of the blades was twisted such than an average incidence angle of 2 degrees existed when the blade was installed on the shaft. These variations were included in the analysis and their effects were found to be significant.

The windmill was mounted on the H-Beam of the tunnel balance system by the use of cylindrical pylons extending from the H-Beam, through the ground board, and connected fore and aft to two 4" steel channels as shown on figure 4. This allowed the use of the tunnel scale system to measure total drag and torque (yaw moment).

INSTRUMENTATION AND EQUIPMENT

The lower portion of the windmill shaft shown on figure 5 was instrumented and contained accessories as follows:

1. A manual, shoe type, automotive brake was installed to prevent rotation during periods of non-testing and transportation.

2. An electrically operated disc brake was provided for stopping rotation under emergency conditions.

3. A motor generator, driven by a V-Belt from a pulley on the lower shaft.

4. A torque sensor, located on the lower shaft between the windmill and the motor generator drive. The torque sensor also include a pick-off to provide shaft speed.

5. An angular position pick-up, located at the bottom of the shaft.

Data was recorded on magnetic tape and simultaneously on oscillograph paper for immediate assessment of test results.

Tunnel conditions and balance parameters were recorded on tunnel facility equipment. These included tunnel velocity, dynamic pressure, model drag, and model yaw moment.

TEST CONDITIONS AND PROCEDURES

The initial test was run at a tunnel wind velocity of approximately 27.3 ft./sec (8.321 m/sec). This test was to determine the variation of windmill power output versus rotation rate. The no load condition was obtained by bringing the tunnel velocity to approximately 14.7 ft./sec (4.481 m/sec) and manually starting the windmill, then raising the free stream velocity to 27.3 ft./sec (8.321 m/sec) and allowing tunnel conditions to become stable prior to recording. All subsequent recordings at test points were under stable conditions. Tunnel velocity was then decreased until the windmill stalled, and the motor generator was coupled with a V-Belt to the windmill. The tunnel velocity was raised and allowed to stabilize at approximately 27.3 ft./sec (8.321 m/sec). The windmill was started with the motor-generator and when it became self sustaining all electrical load was removed. Data was recorded under the no load condition.

Voltage was applied to the field of the generator until the load caused the windmill rotation rate to decrease by about 20 RPM. Sufficient time was allowed for test conditions to become stable and data was taken for approximately 10 secs. This procedure was repeated with increments in RPM of about 20, until the applied load exceeded the windmill capacity. The power was dissipated in a resistor bank.

A second test was run at a free-stream velocity of approximately 22.7 ft./sec (6.919 m/sec) and the previously outline sequence of events at 27.3 ft./sec (8.321 m/sec) free-stream velocity were repeated.

The area upstream of the windmill was surveyed with a 3 probe rake, also a duplicate survey was made downstream. These surveys were made with the windmill not rotating and the blades locked normal to the free-stream direction, at a free-stream velocity of approximately 29.3 ft./sec (8.931 m/sec). An additional survey was made downstream with the windmill operating at approximately peak efficiency. Figure 6 shows a grid of probe locations used for the surveys, and figure 7 shows the velocity profiles of these surveys where (a) is the profile across the tunnel at the windmill horizontal centerline, and (b) is the survey profile at the vertical centerline.

It is interesting to note that the velocity defect directly downstream of the windmill shaft is observable even when the windmill is operating near maximum efficiency.

RESULTS AND DISCUSSION

The primary purpose of this test program was to obtain power coefficient, C_p as a function of the windmill tip speed-wind velocity ratio, R. The power coefficient is defined as the ratio of the actual windmill power output to the total power available in the free stream flow passing through the area swept by the windmill. The tip speed ratio, R, is defined as the ratio of blade velocity at the point of maximum radius to the free stream wind velocity. In terms of measured quantities these can be written as follows:

$$C_p = \frac{\pi \, TN}{30 \, q_\infty \, A \, V_\infty} , \tag{1}$$

and

$$R = \frac{r_{max} \, N}{30 \, V_\infty}, \tag{2}$$

A summary of test conditions and measured output is given in Table I. Included in the table are tunnel velocity windmill RPM, and average shaft torque over a 5 second time period. To determine the variation in velocity within the test section a survey of the tunnel in the region just upstream of the windmill was made. These results indicated an essentially uniform velocity existed in the region of the windmill with an average variation of about 2%. The wind velocities given in Table I were obtain from a single fixed probe measuring dynamic pressure as described in reference 1.

Power Coefficient. - Figure 8 is a graphic representation of C_p Vs R. The solid line shows results of a nominal NACA 0012 airfoil used in the analysis and the dashed line represents the analytical results corrected for misalinement, roughness, etc. The data points shown are recorded from two series of test points. In one series the wind tunnel free-stream velocity was approximately 22.7 ft/sec (6.919 m/sec), the second at approximately 27.3 ft/sec (8.321 m/sec). It can be seen that good agreement exists between analytical and test results. Also shown on this curve are the data from reference 3.

The differences between the two sets of measured data is significant and possibly due to differences in blade quality. As previously indicated, the blade on the test configuration varied somewhat from the idealized blade. When a nominal NACA 0012 airfoil is used in the analysis the performance of the windmill is considerably improved as indicated by the solid curve of figure 8.

Drag Coefficient. - A major factor in determining windmill performance at high tip speed ratios is the zero lift drag coefficient, C_{D_o}. This quantity determines the no load tip speed ratio at which a given configuration will operate. A value of $C_{D_o} = .0083$ was used in the analysis and it was found that increasing this value to about $C_{D_o} = .014$ would cause the computed no load tip speed ratio to agree favorably with the measured value. The performance characteristics at low tip speed ratios are dependent on the stall characteristics of the airfoil section. The angle of attack at which stall occurs directly determines the tip speed ratio at which the windmill is capable of producing power. For the tested configuration the lower no load tip speed ratio was about 2.5 to 3.0. It was very difficult to obtain data points once stall begins to occur on a major portion of the blade.

Torque Coefficient. - Figure 9 shows the torque coefficient variation through a shaft rotation of 12 π radians (6 revolutions) for each of the test runs. The torque coefficient C_T is given by

$$C_T = \frac{T}{r_{max}\,(q_\infty A)} \tag{3}$$

A phenomena was observed in these data that has not been satisfactorily explained to date. Theoretically, the variation of aerodynamic torque with position is cyclic with period of one half of a revolution for a 2 bladed design, and the amplitude is a function of the tip speed ratio. When friction losses and inertial effects are considered the variations in amplitude tend to be reduced and the result should be a curve which approaches the average torque value but which still maintains its cyclic character.

As can been seen from the data on figure 9 the torque curve does vary in a cyclic manner with Θ, however, the period is 6π rather than π. The behavior is most pronounced in those runs during which the windmill was operating near maximum efficiency, for example runs 18 and 22. Nothing has been identified in the mechanical systems that would cause the effect that has been identified with the exception of the torque sensor itself, and analysis of the torque sensor has indicated that it could not have caused the problem. (One possibility is that some type of coupling existed between the tunnel drive system and the windmill that results in a one per 6 cycle excitation).

Shown on figure 10 is the drag coefficient versus tip speed ratio. The drag coefficient is represented by an envelope due to low values of drag compared to the normal operating range of the tunnel balance system. Measured values of drag fell within the tolerance band. The tare drag of the windmill at R = 0 has been subtracted from the total drag measurement. The computed drag is also shown as a solid curve. Good agreement was obtained at lower values of tip speed ratio but at higher values the analysis overpredicts drag.

Also measured was the total system torque (yaw moment). These data matched the general trend of the power coefficient curve shown on figure 8 when appropriately transformed, however, the magnitude did not agree. This was due to the fact that the measured yaw moments included a tare value due to asymmetries in the support structure. This tare value was measured, however, its magnitude was so small that it was below the tolerance band on yaw moment. Since these data could not be corrected, they are not presented in this report.

CONCLUSIONS

A 14' diameter Darrieus type windmill with catenary shape blades using a nominal NACA 0012 airfoil section has been tested in the LaRC Full Scale Wind Tunnel. Results from these tests indicate the efficiency is somewhat less than that cited in reference 6. This reduction in efficiency can be attributed to variations in the blade profile from the NACA 0012 design, and also to misalignment of the blades with respect to the shaft such that the blade chord was at an angle to the tangential velocity components. The peak efficiency of the tested configuration is about 25% lower than that of a high performance horizontal axis experimental windmill, however, it is felt that with better control on manufacturing procedures the difference could be reduced to less than 10%.

REFERENCES

1. Darrieus, G. J. M: U.S. Patent No. 1,835,018, December 8, 1931.

2. South, P.; and Rangi, R. S.: Preliminary Tests of a High Speed Vertical Axis Windmill Model. LTR-LA-74, National Research Council, Canada, March 1971.

3. South, P.; and Rangi, R. S.: A Wind Tunnel Investigation of a 14 Ft. Diameter Vertical Axis Windmill. LTR-LA-105, National Research Council, Canada, September 1972.

4. Muraca, R. J.; Stephens, M. V.; and Dagenhart, J. R.: Theoretical Performance of Cross-Wind Axis Turbines. TMX-72662.

5. De France, Smith J.: The NACA Full-Scale Wind Tunnel. TR-459, 1933.

6. Armstrong, David H.; and Kirby, Cecil E.: A Residential Size Vertical Axis Windmill Design, TMX-72770.

TABLE I

RUN NO.	V_∞ FT/SEC, (m/sec)		WINDMILL R.P.M.	AVERAGE TORQUE IN-LBS, (n, m)		C_p	R
10	27.359	(8.339)	325.00	0	0	0	8.72
11	27.359	(8.339)	307.69	80.961	(9.213)	0.0662	8.244
12	27.050	(8.245)	283.02	181.985	(20.710)	.1415	7.670
13	27.205	(8.292)	262.01	292.811	(33.333)	.2073	7.060
14	27.817	(8.479)	244.90	402.408	(45.794)	.2481	6.430
15	27.359	(8.339)	220.59	481.345	(54.777)	.2820	5.910
16	27.513	(8.386)	212.77	524.015	(59.633)	.2912	5.669
17	27.359	(8.339)	203.39	570.479	(64.921)	.3082	5.450
18	27.664	(8.432)	192.31	619.471	(70.496)	.3061	5.096
19	27.968	(8.525)	200.00	585.797	(66.664)	.2913	5.242
20	27.817	(8.479)	181.20	652.704	(74.278)	.3000	4.791
21	24.263	(7.395)	172.91	421.254	(47.939)	.2774	5.224
22	24.263	(7.395)	155.44	473.417	(53.875)	.2802	4.696
105	23.019	(7.016)	254.24				
106	22.835	(6.960)	240.00	124.974	(14.222)	0.1370	7.704
107	22.650	(6.904)	222.22	191.491	(21.792)	.1992	7.192
108	22.835	(6.960)	208.33	249.739	(28.420)	.2377	6.688
109	23.019	(7.016)	192.31	310.244	(35.306)	.2661	6.124
110	23.019	(7.016)	175.95	370.544	(42.168)	.2907	5.603
111	23.019	(7.016)	160.00	421.765	(47.997)	.3009	5.095
112	23.019	(7.016)	144.23	450.670	(51.286)	.2899	4.593
113	23.019	(7.016)	135.14	445.364	(50.682)	.2684	4.304

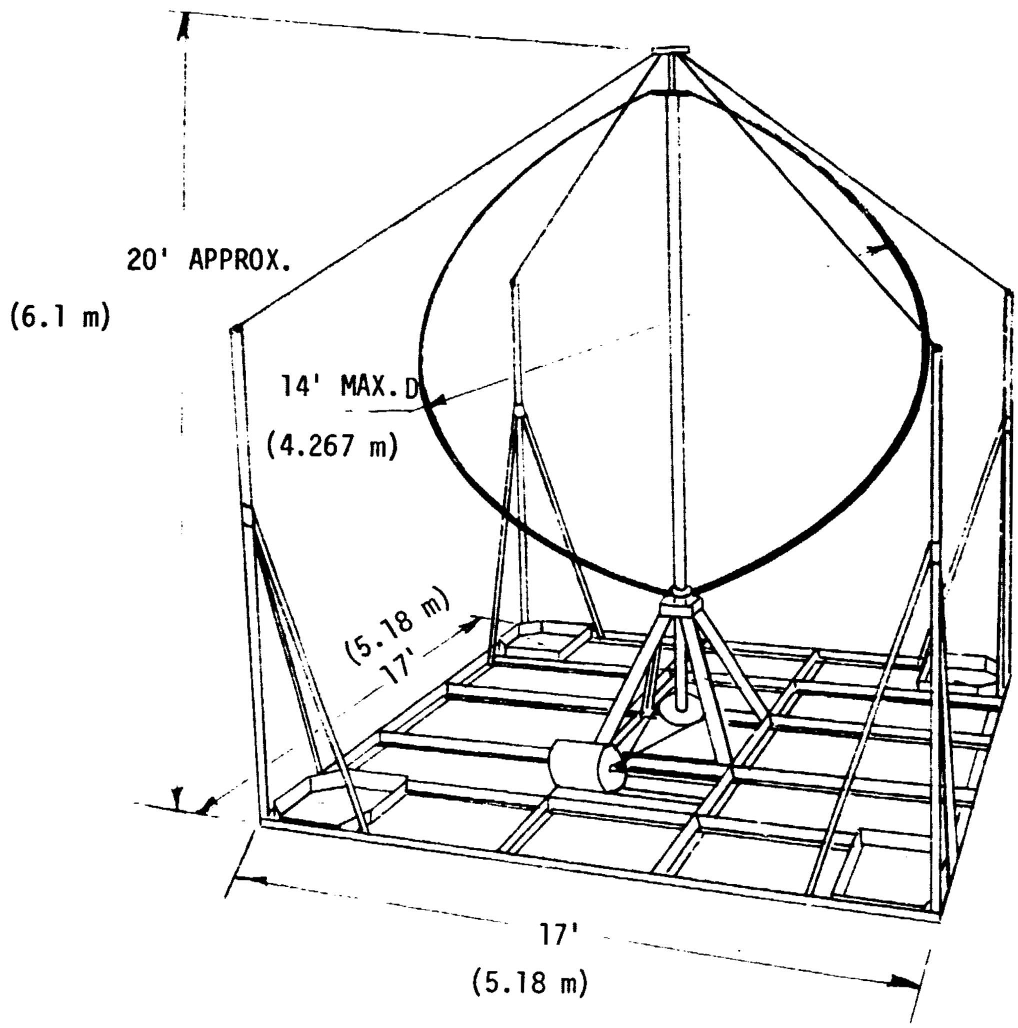

FIGURE 1. - 14' VERTICAL AXIS WINDMILL TEST ASSEMBLY.

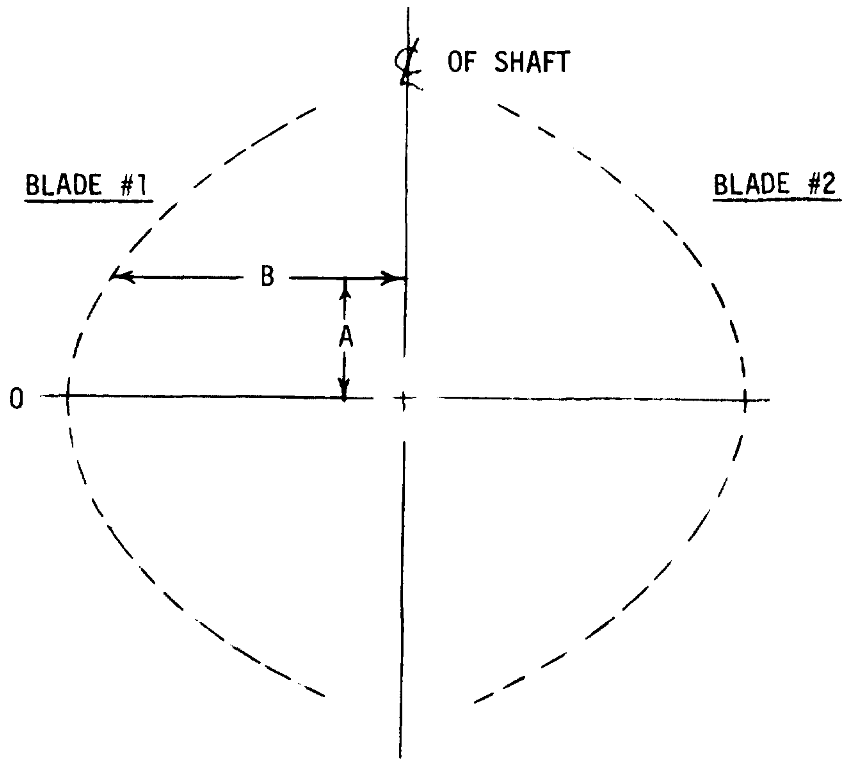

A, m	B, m	
	BLADE 1	BLADE 2
1.8288	.6302	.6556
1.5240	1.0966	1.1494
1.2192	1.4827	1.5256
.9144	1.7590	1.7907
.6096	1.9558	1.9241
.3048	2.0701	2.0812
0	2.1177	2.1146
-.3048	2.0923	2.0828
-.6096	1.9955	1.9780
-.9144	1.8177	1.7971
-1.2192	1.5558	1.5240
-1.5240	1.1859	1.1557
-1.8288	.6826	.6509

FIGURE 2. - PHYSICAL DIMENSIONS OF THE TEST 14' CATENARY

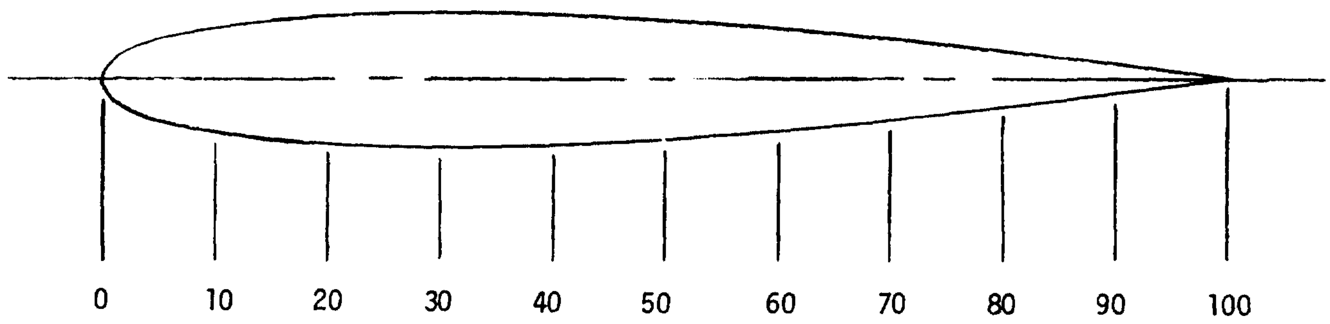

STA. %	*ORD. %	STA. %	ORD. %	STA. %	ORD. %
0	0	15	5.345	60	4.563
1.25	1.894	20	5.738	70	3.664
2.50	2.615	25	5.941	80	2.623
5.0	3.555	30	6.002	90	1.448
7.5	4.200	40	5.803	95	.807
10.0	4.683	50	5.294	100	.126

L. E. RADIUS = 1.58%

* SYMMETRICAL AIRFOIL

FIG. 3. NACA 0012 AIRFOIL SECTION

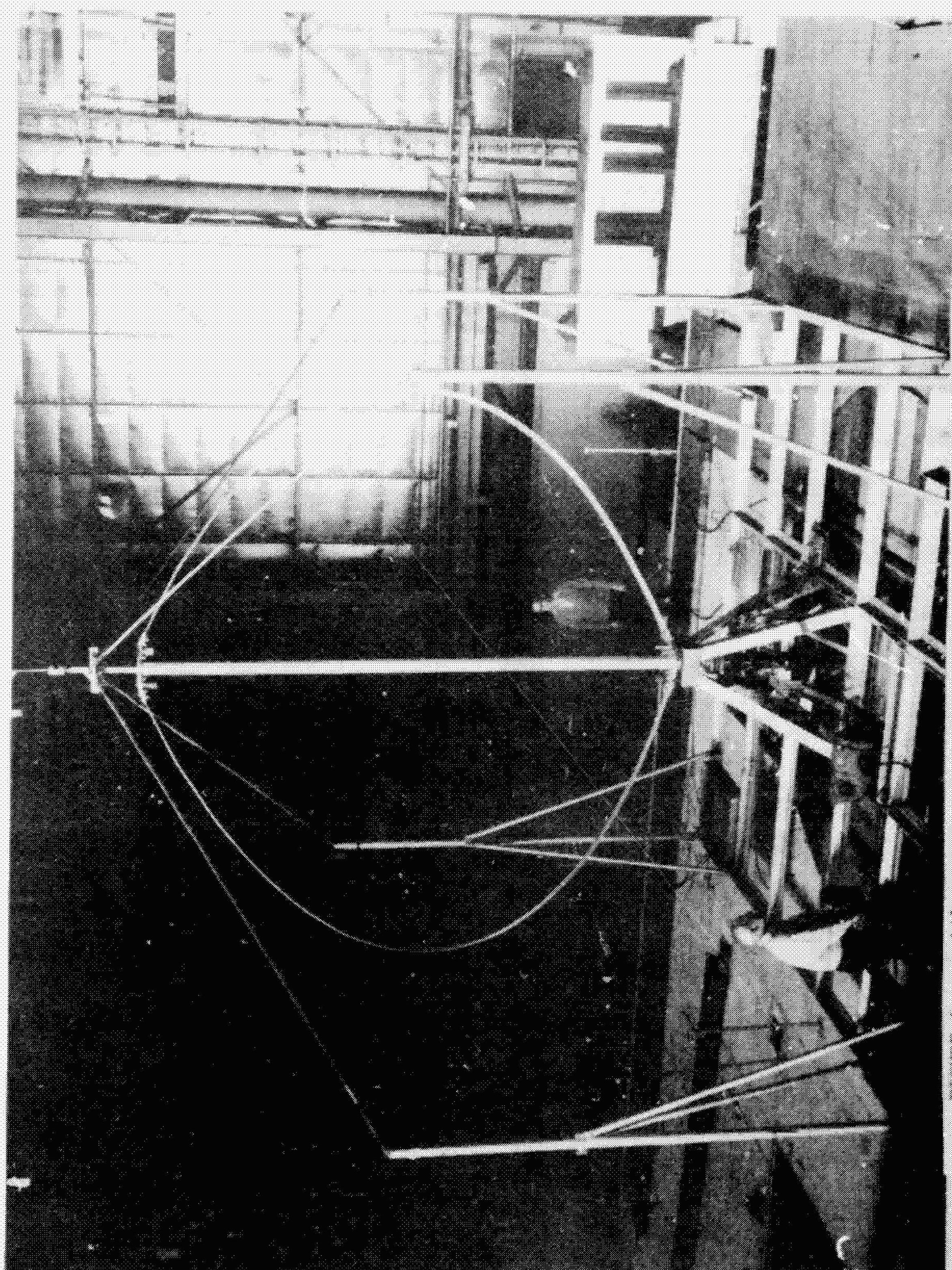

FIGURE 4. — 14' VERTICAL AXIS WINDMILL MOUNTED IN THE FULL SCALE WIND TUNNEL.

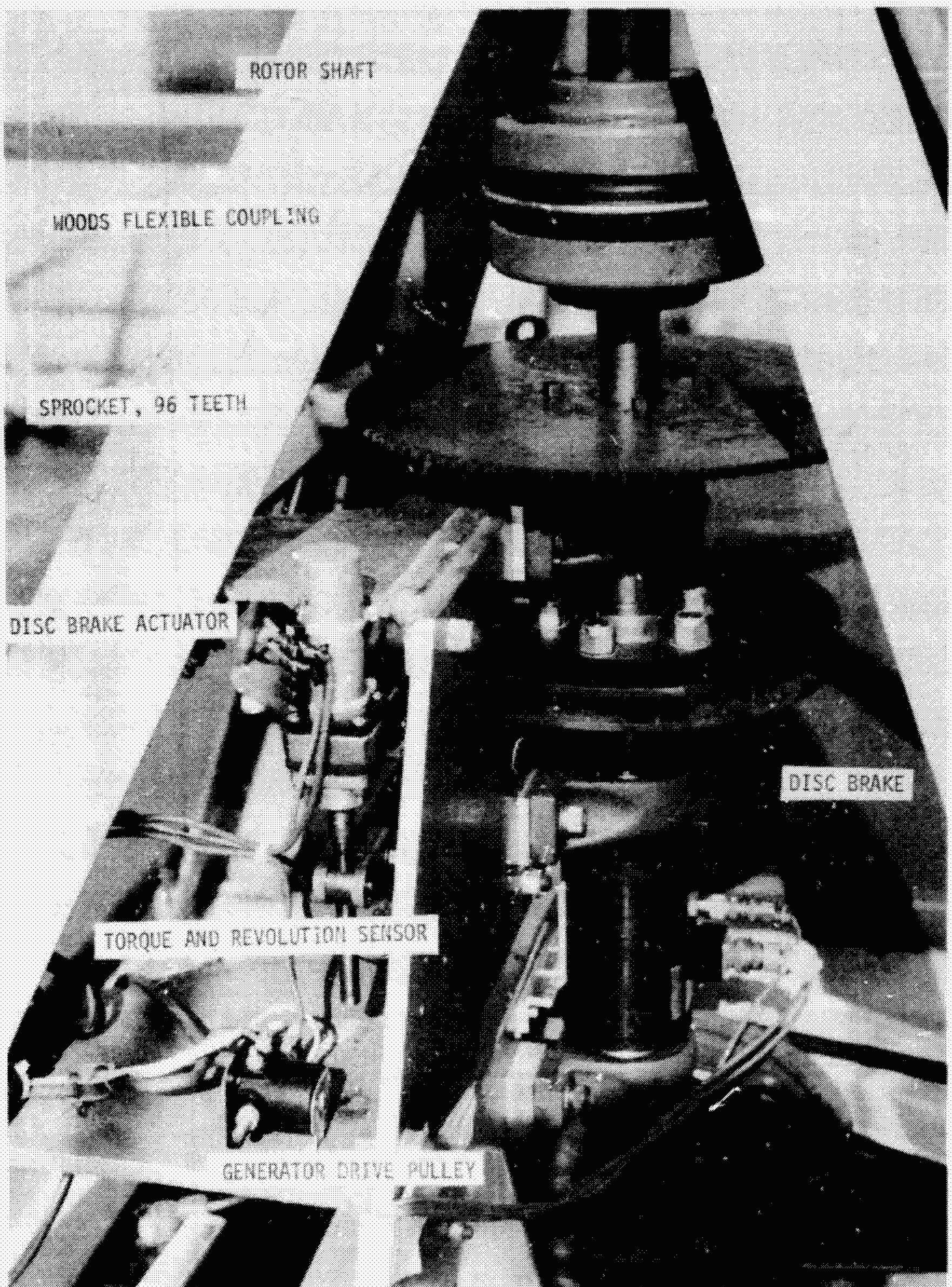

FIGURE 5. - INSTRUMENTATION OF 14' VERTICAL AXIS WINDMILL

ORIGINAL PAGE IS
OF POOR QUALITY

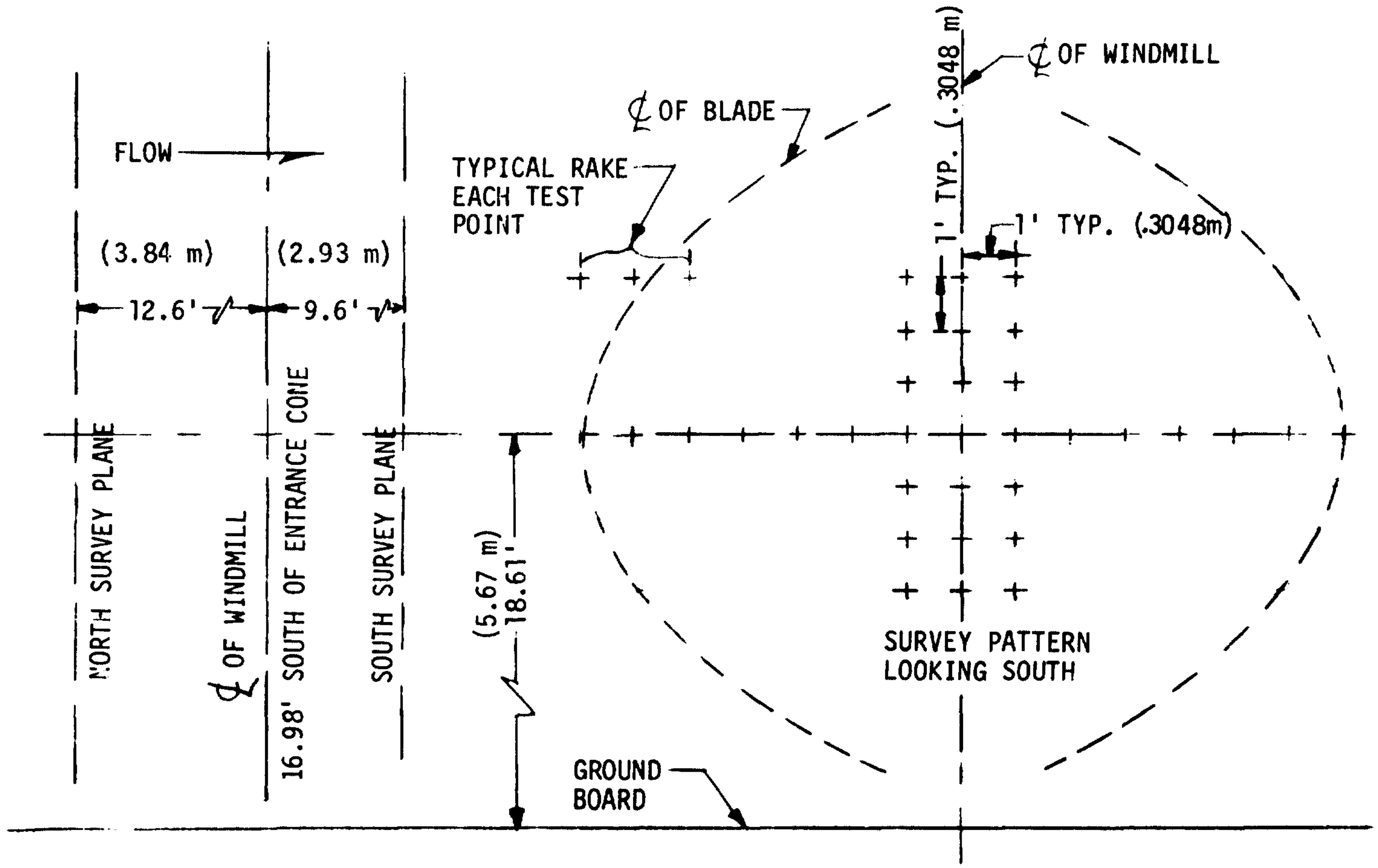

FIG. 6. WIND TUNNEL SURVEY PROBE LOCATIONS

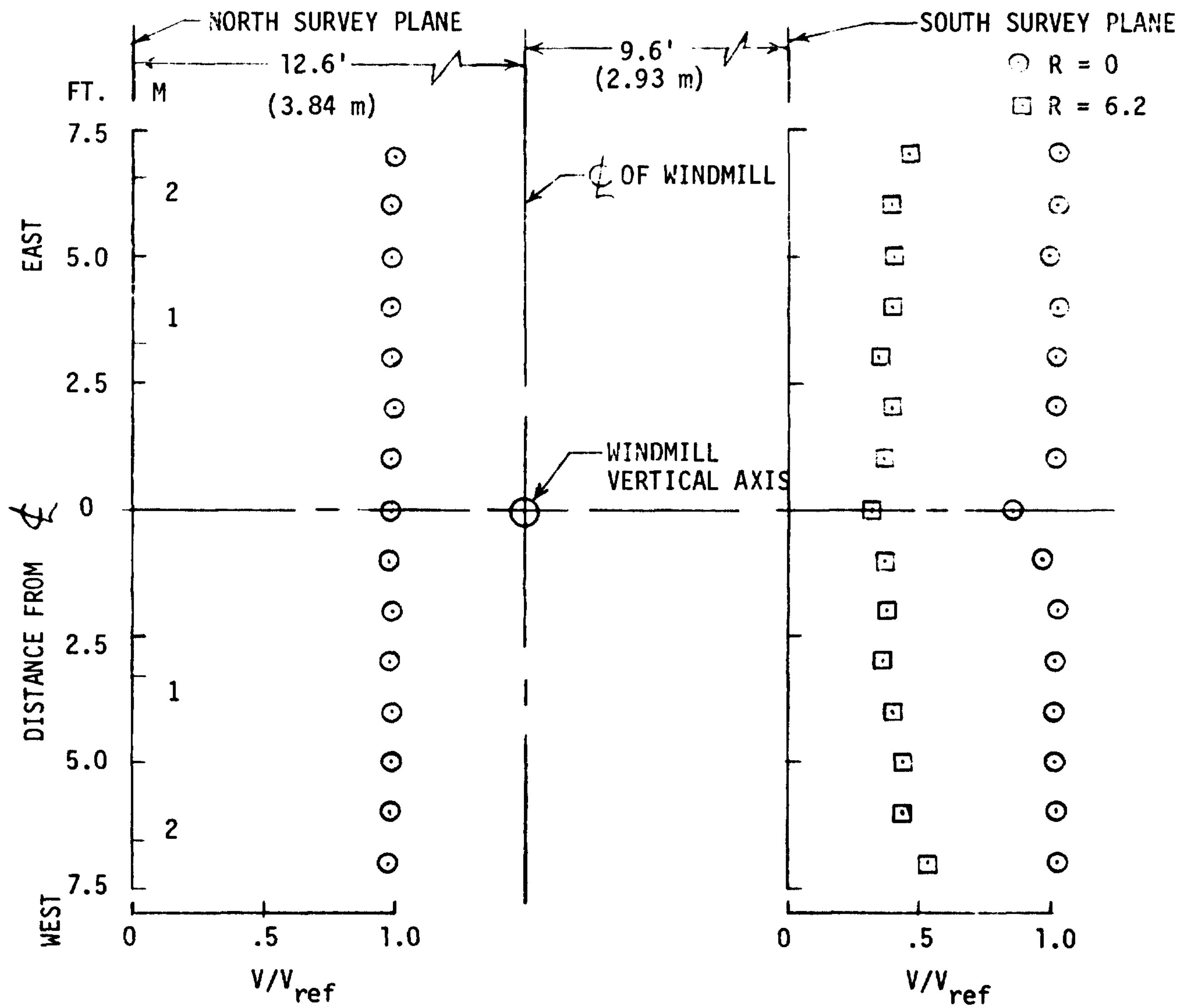

FIG. 7. VELOCITY PROFILES, (a) ACROSS THE WIND TUNNEL AT THE WINDMILL CENTERLINE.

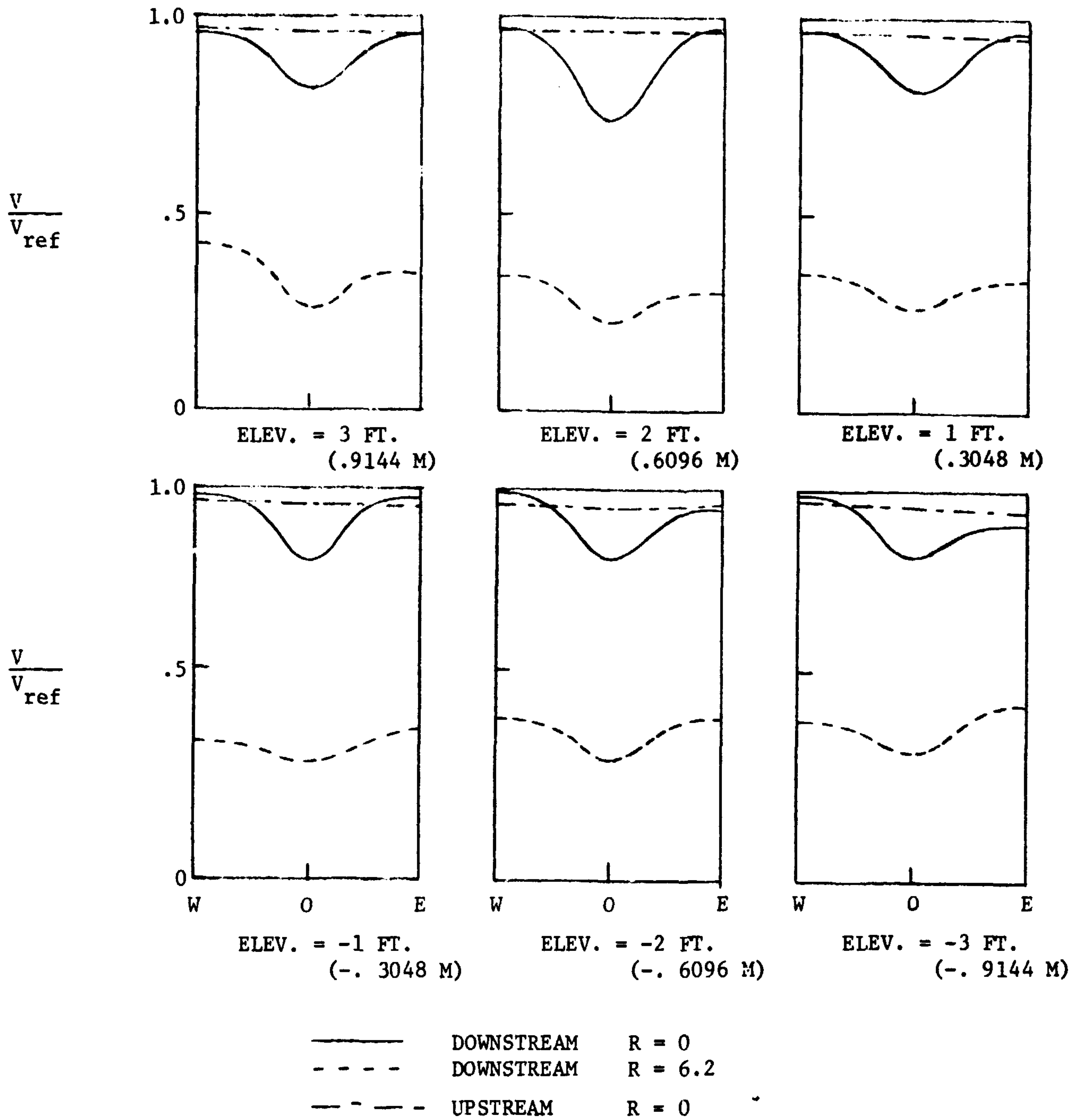

ELEVATIONS MEASURED FROM HORIZONTAL CENTERLINE OF WINDMILL

HORIZONTAL PROBES ARE ON CENTERLINE AND 1 FT. (.3048 M) EAST AND WEST OF CENTERLINE

FIGURE 7. - VELOCITY PROFILES, (b) SURVEY AT VERTICAL CENTERLINE OF WINDMILL

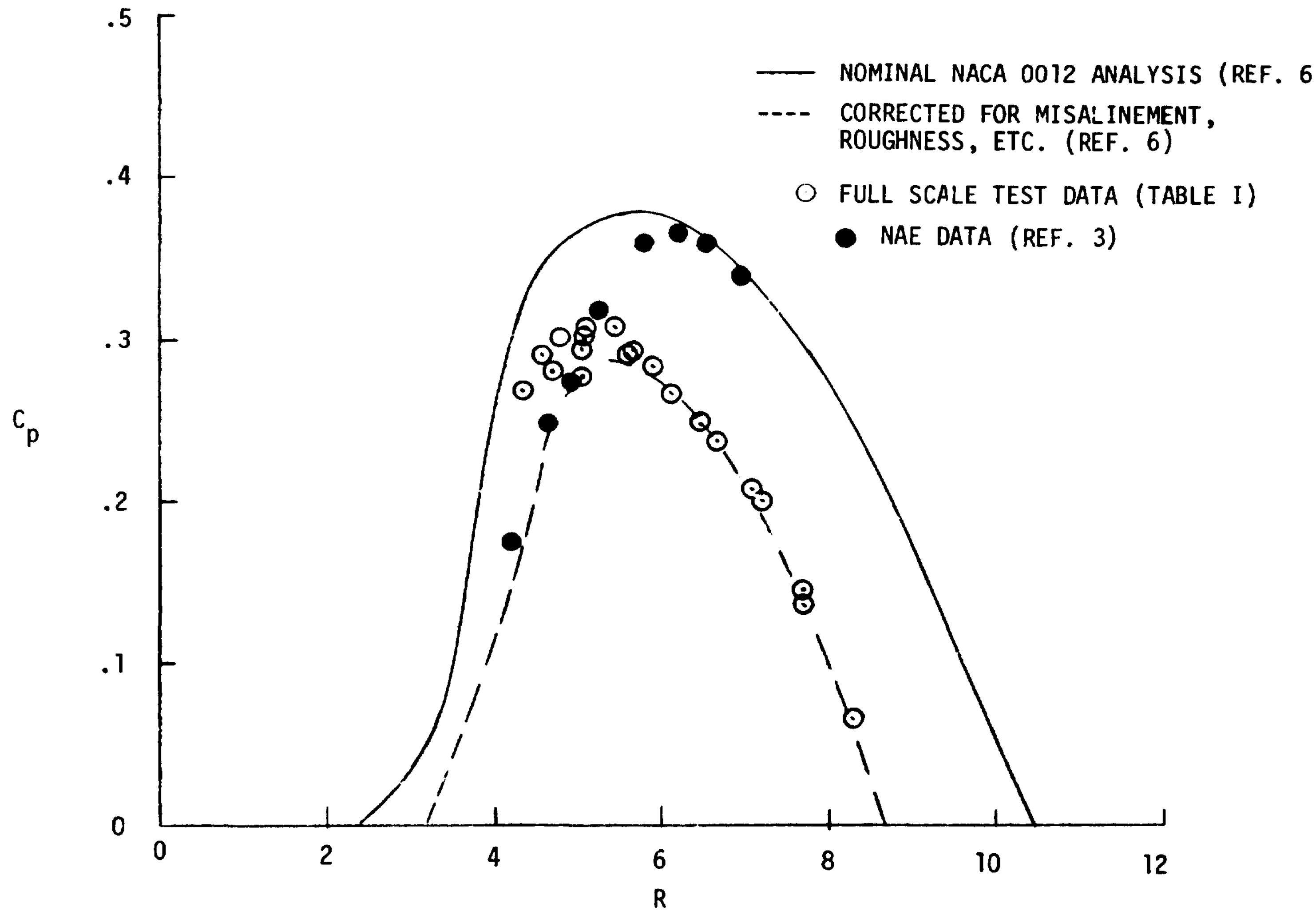

FIG. 8. POWER COEFFICIENT VS TIP SPEED-FREE STREAM VELOCITY RATIO

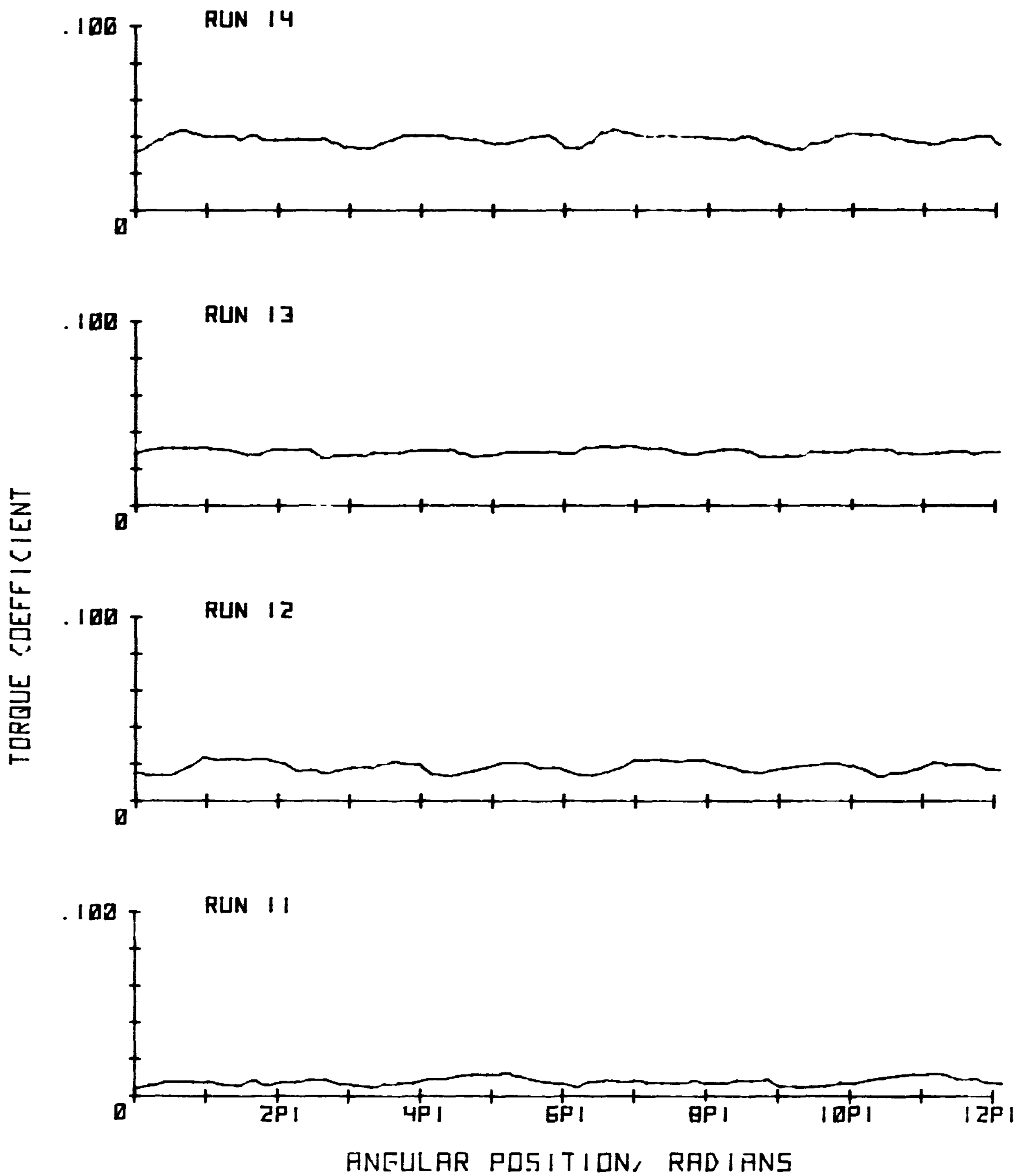

FIG. 9. TORQUE COEFFICIENT VERSUS ANGULAR POSITION

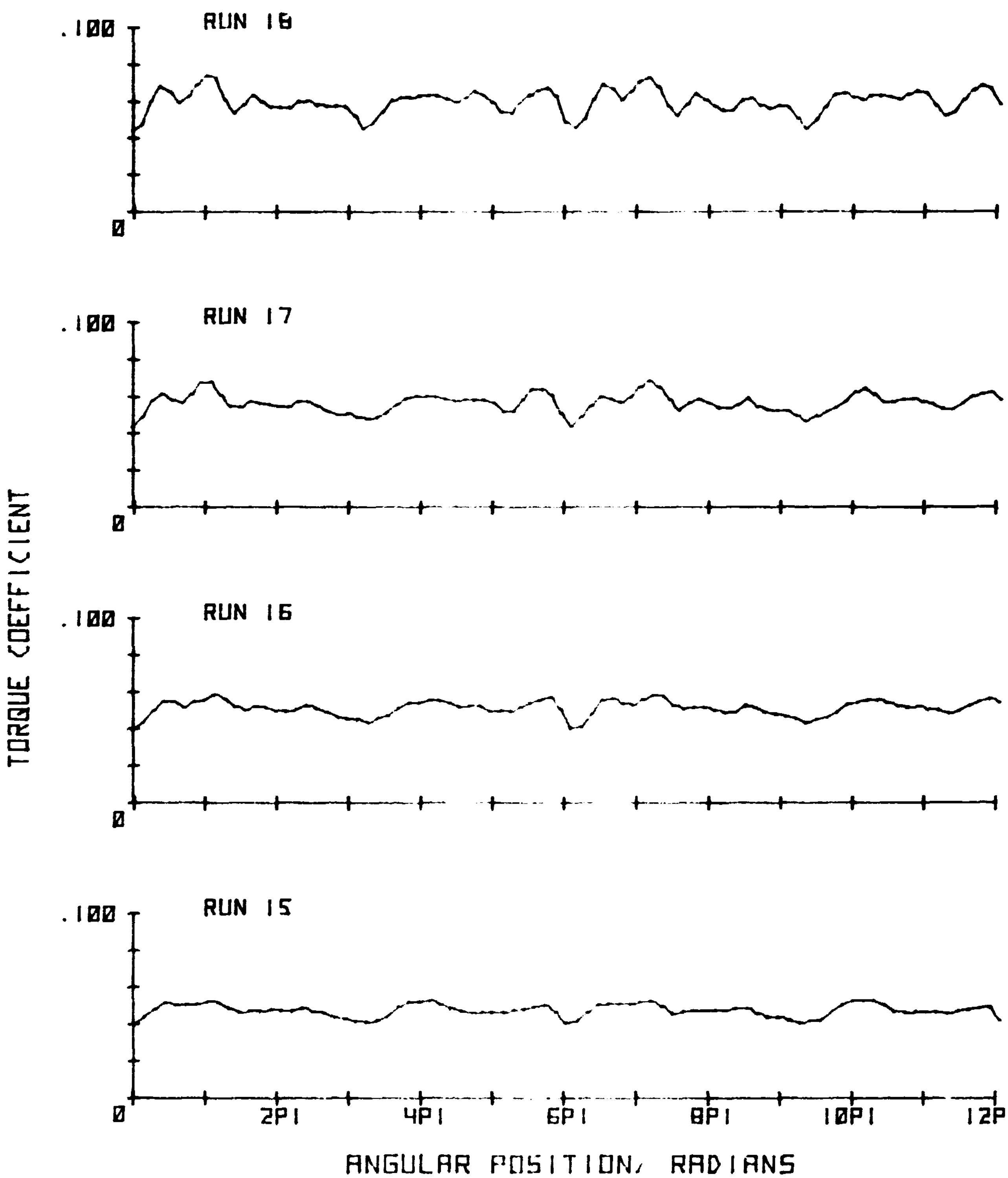

FIG. 9. CONTINUED
TORQUE COEFFICIENT VERSUS ANGULAR POSITION

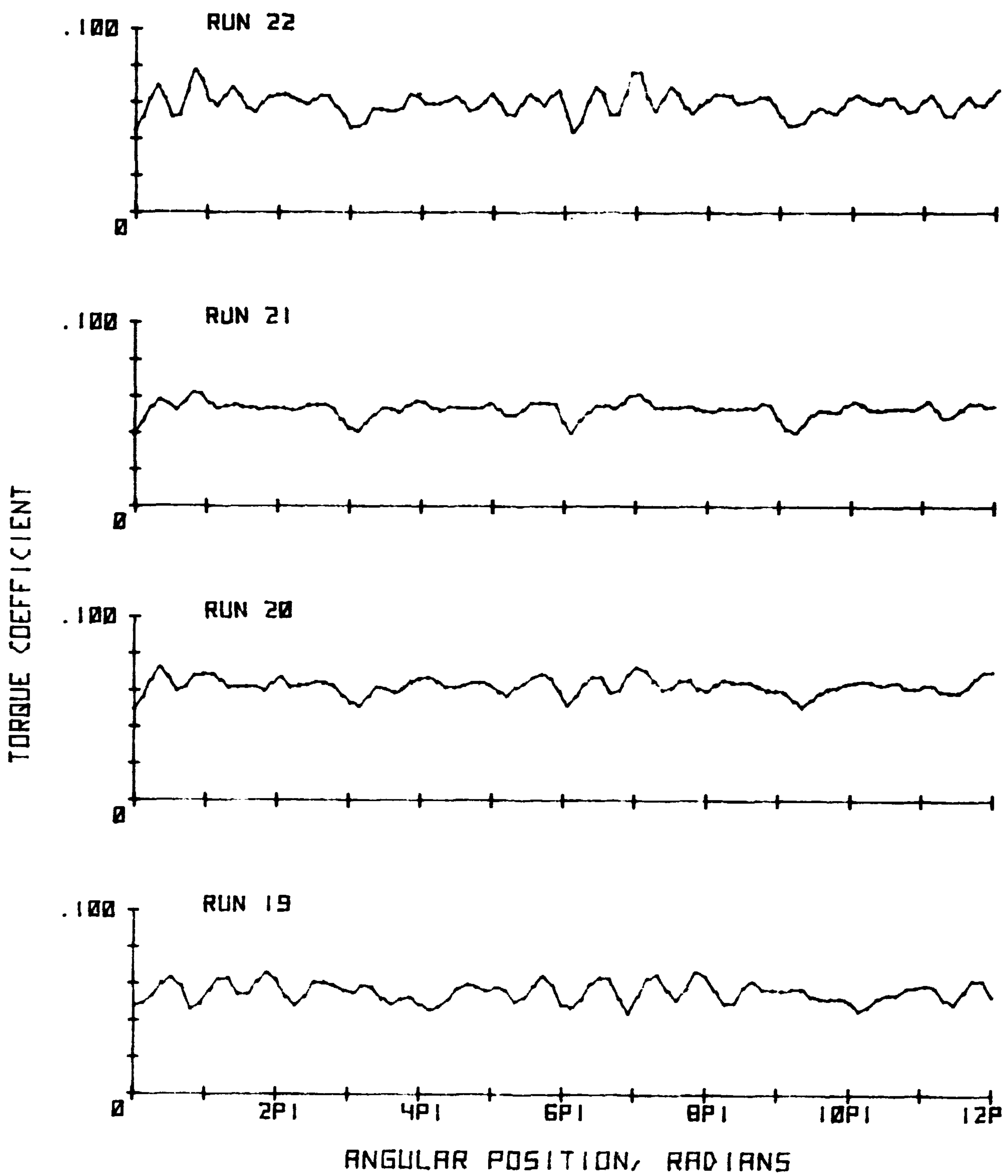

FIG. 9. CONTINUED

TORQUE COEFFICIENT VERSUS ANGULAR POSITION

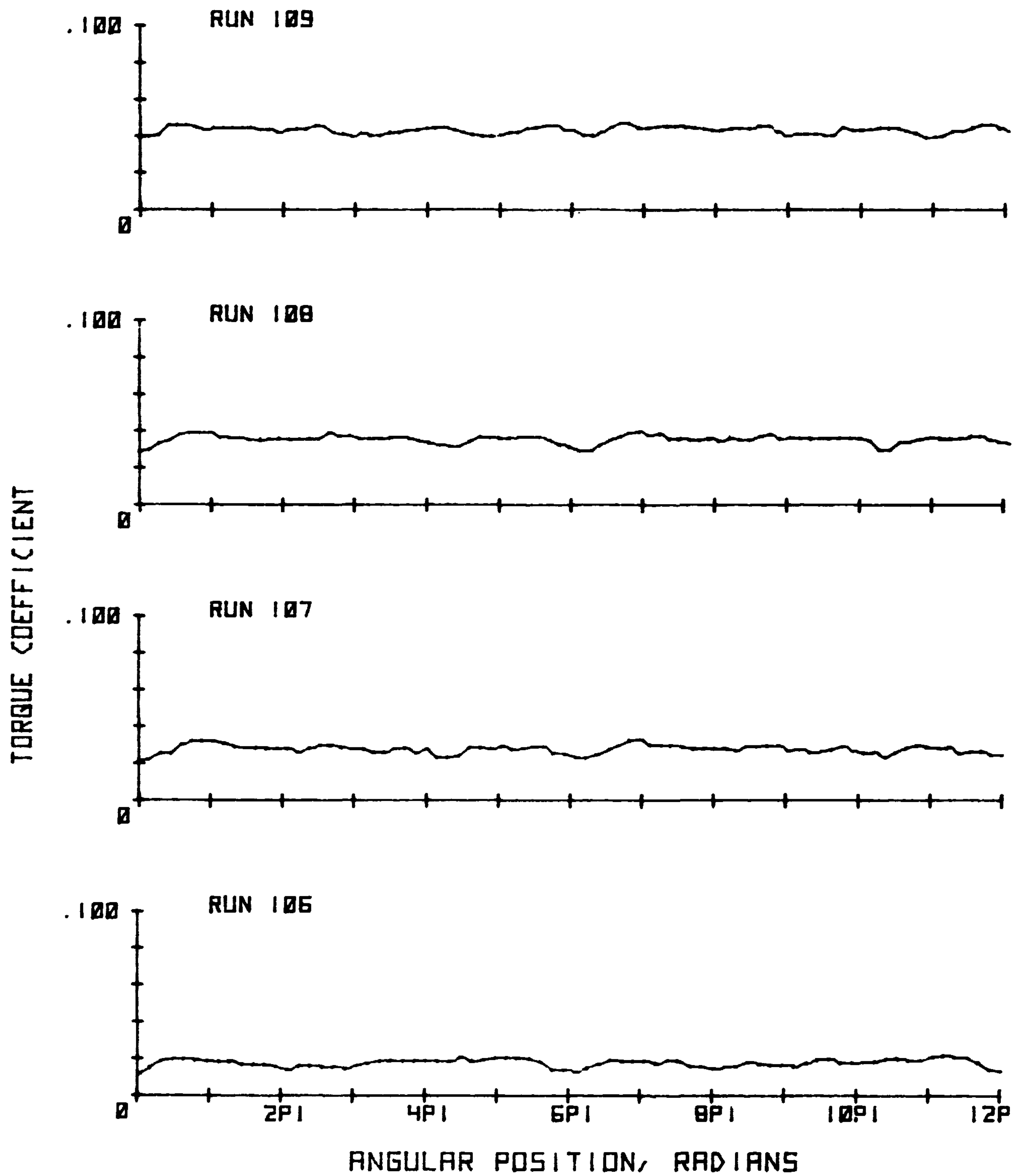

FIG. 9. CONTINUED

TORQUE COEFFICIENT VERSUS ANGULAR POSITION

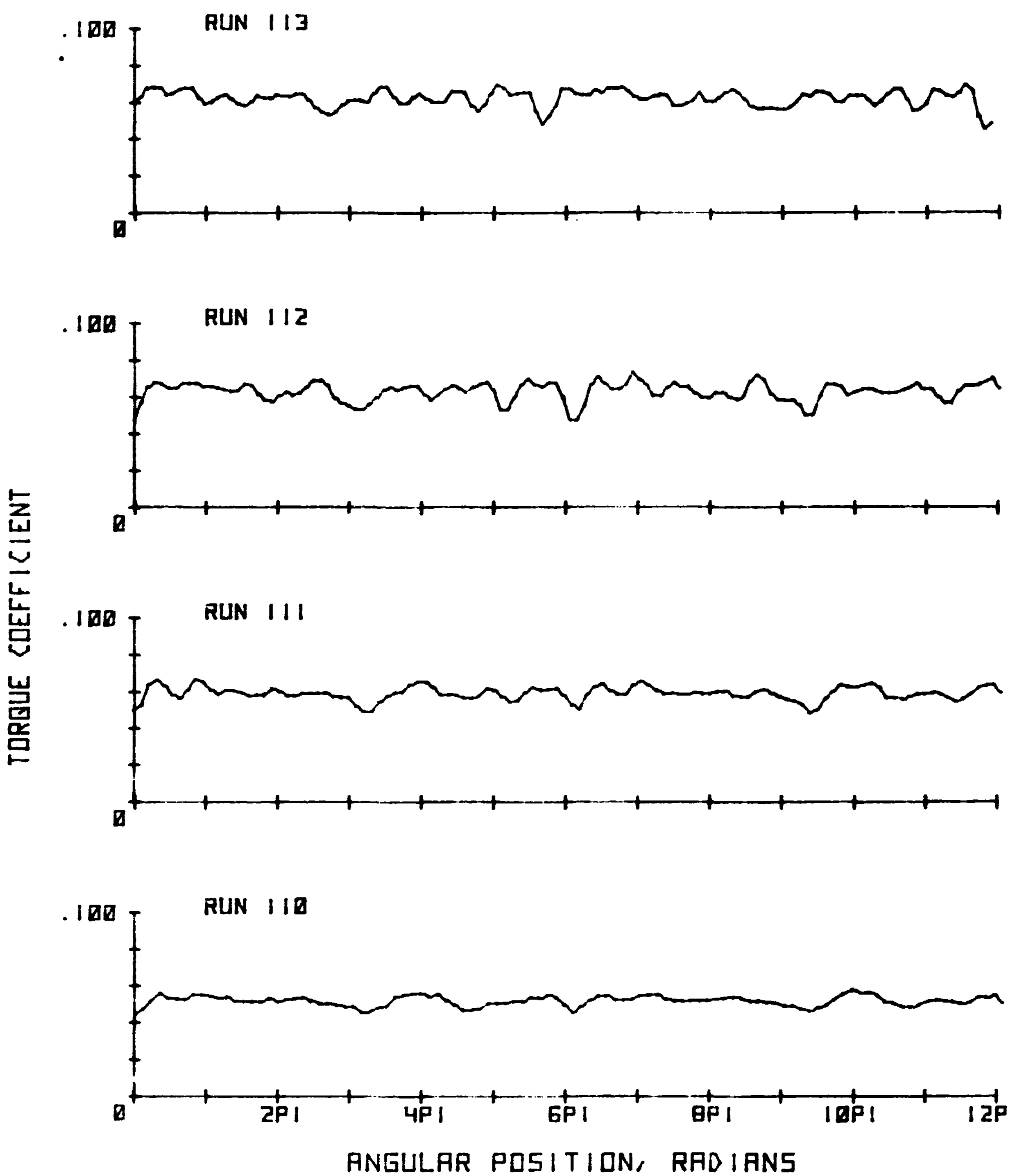

FIG. 9. CONCLUDED

TORQUE COEFFICIENT VERSUS ANGULAR POSITION

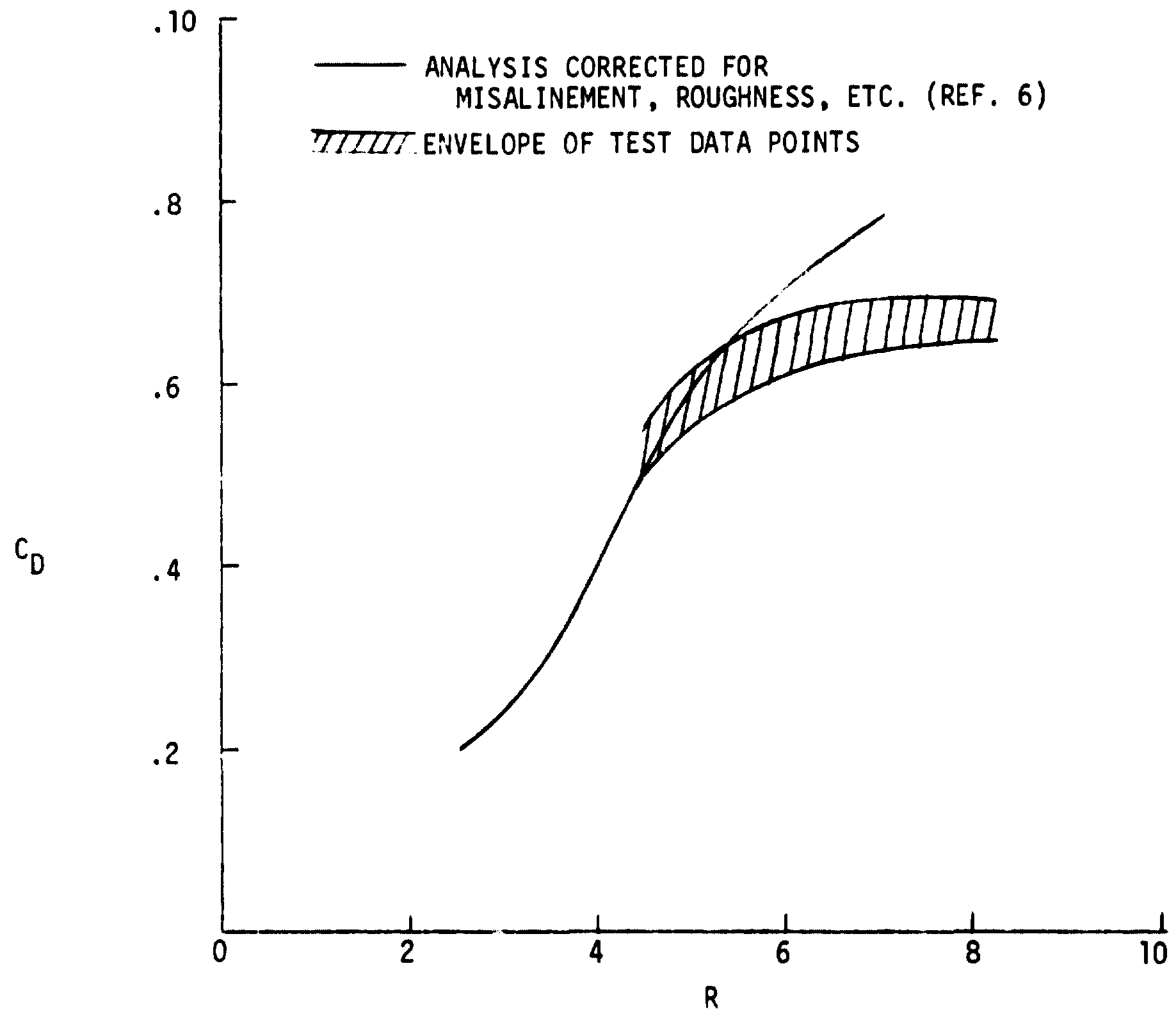

FIG. 10. DRAG COEFFICIENT VERSUS TIP-SPEED-FREE STREAM VELOCITY RATIO.